

# B22

*by* Maria Ulfa

---

**Submission date:** 30-May-2023 07:54PM (UTC-0500)

**Submission ID:** 2105612693

**File name:** Lampiran\_B22.pdf (1.48M)

**Word count:** 4930

**Character count:** 25118

RESEARCH ARTICLE | JUNE 04 2020 <sup>3</sup>

## Density functional and perturbation calculation on the corrosion inhibition performance of benzylnicotine and its derivatives **FREE**

S. Hadisaputra ✉; A. A. Purwoko; Y. Wirayani; ... et. al

 Check for updates

*AIP Conference Proceedings* 2243, 020006 (2020)  
<https://doi.org/10.1063/5.0001077>



View  
Online



Export  
Citation

CrossMark

### Articles You May Be Interested In

Density functional study of heteroatoms effect on corrosion inhibition efficiency of methenamine and its derivatives <sup>3</sup>

*AIP Conference Proceedings* (April 2023)

Mangosteen peel extract as a green corrosion inhibitor of mild steel in 1 m hydrochloric acid: Gravimetric, quantum chemical, and Monte Carlo simulation studies

*AIP Conference Proceedings* (August 2022)

Investigation of some phenolic-type antioxidants compounds extracted from biodiesel as green natural corrosion inhibitors; DFT and molecular dynamic simulation, comparative study

*AIP Conference Proceedings* (December 2019)



Time to get excited.  
Lock-in Amplifiers – from DC to 8.5 GHz

[Find out more](#)

 Zurich  
Instruments

# Density Functional and Perturbation Calculation on The Corrosion Inhibition Performance of Benzylnicotine and Its Derivatives

S. Hadisaputra<sup>1, a)</sup>, A. A. Purwoko<sup>1</sup>, Y. Wirayani<sup>2</sup>, M. Ulfa<sup>2</sup>, S. Hamdiani<sup>2</sup>

<sup>1</sup>Chemistry Education Division, Faculty of Teacher Training and Science Education, University of Mataram, Indonesia

<sup>2</sup>Department of Chemistry, Faculty of Mathematic and natural Science, University of Mataram, Indonesia

<sup>a)</sup>Corresponding author: rizal@unram.ac.id

**Abstract.** The search for corrosion inhibitors based on natural products that are environmentally friendly with high inhibition efficiency is still the focus of current research. The corrosion inhibition efficiency of nicotine and its derivatives has been studied using DFT and *ab initio* MP2 method. This research focuses on the use of electronic parameters and the natural bond analysis approach to explain the corrosion inhibition performance of nicotine and its derivatives. The electronic properties of molecules, including the frontier molecular orbitals (HOMO and LUMO energy), ionization potential, electron affinity, electronegativity, number of electron transfer from inhibitors to metal and interaction energy have a strong relationship with inhibition performance. Interaction mechanism is obtained from natural bond between inhibitors with iron metal in more detail. The presence of electron donor groups within the framework of inhibitors show significant contribution toward the corrosion inhibition performance.

## INTRODUCTION

Corrosion prevention is urgently required because the corrosion process causes considerable economic losses. The use of corrosion compounds based on organic compounds is an effective and efficient method for the prevention of corrosion. Organic compounds have effectiveness as corrosion inhibitors due to the presence of heteroatom groups (O, N, S, and P) and the existence of  $\pi$  electron donors from their double or aromatic bonds [1-4].

Nicotine and its derivatives meet the criteria as a good organic compound based corrosion inhibitor. Many experimental studies indicate that nicotine compounds are potential to be developed as corrosion inhibitors. Ju and Li reviewed the efficiency of inhibiting nicotine against zinc and alloys under acidic conditions. The inhibition efficiency of nicotine corrosion from this experiment was 96.6% [3]. Nicotine inhibition efficiency in HCl medium against iron solids was 90.8% [4]. Another study by Zhao *et al.* [5] showed that the inhibition efficiency of nicotine and its derivatives in steel N80 in a solution of 10% HCl was 92%. Sigh *et al.* combined theoretical and experimental studies to study the corrosion inhibition efficiency of 4-(N,N-dimethylamino) benzaldehyde nicotinic hydrazone against mild steel in 1 M HCl. Sigh *et al.* reported a good correlation between theoretical studies and experiments in explaining corrosion inhibition efficiency and corrosion inhibition mechanism by the nicotine derivatives [5].

Theoretical studies have proven to be effective in bridging the difficulties found in experimental studies. The electronic parameters of the inhibitor that are most relevant to the increase in corrosion inhibition efficiency can be explained very well using theoretical studies. Many theoretical studies have been carried out to test the efficiency of corrosion inhibition. The theoretical study was able to show a good correlation between the electronic parameters of organic compounds and their corrosion inhibition efficiency. Theoretical studies are also able to explain the mechanism of inhibition of corrosion by organic molecules on metal surfaces [6-13]. In this report, the influence of electron donating and withdrawing substituent on the corrosion inhibition performance of nicotine and its derivatives was studied using the *ab initio* MP2 and DFT methods. The effect of substituent donors and electron

1 attractors is presented in the form of correlations between molecular electronic parameters and corrosion inhibition efficiency. The Fukui index and natural bond orbital (NBO) analysis are used to show the contribution of each donor atom from the substituent to increase the efficiency of corrosion inhibition. The effect of back donation from metals to inhibitors is also presented showing details of the interaction between inhibitors and metal surfaces.

### Computational Method

Theoretical calculations of the inhibitory ability of corrosion of nicotine compounds and their derivatives were obtained using density functional theory and *ab initio* MP2 calculations. All calculations were performed using Gaussian 09 software [14]. The base set of 6-311G(d,p) and the LANL2DZ ECP combination are used referring to the suitability of theoretical and experimental data on the system being studied. The polarized continuum model (PCM) was used to apply the solvent system because the dominant corrosion occurred in the solvent. Optimization of inhibitor structure was not carried out in solvents because it would only have a minimal effect on structural parameters and electronic energy [15-18].

Theoretically, the calculation of ionization potential (I) and electron affinity (A) uses the theorem that Koopman developed [19]. Koopman's theorem explains the relationship between ionization potential (I), electron affinity (A), electronegativity ( $\chi$ ),  $E_{\text{HOMO}}$  and  $E_{\text{LUMO}}$  energy as the following formula:

$$I = -E_{\text{HOMO}} \quad 1$$

$$A = -E_{\text{LUMO}} \quad 2$$

$$\chi = \frac{I+A}{2} \quad 3$$

The Pearson method provides a way of calculating fraction of electron transfer ( $\Delta N$ ) between inhibitor molecules and metal surfaces. According to Pearson, when a system with different electronegativity has contact, the electrons will flow from a low-electronegativity system to a system with high electronegativity. This electron flow stops when the chemical potential of the two systems becomes the same. To calculate fraction of electron transfer, the theoretical electronegativity value of iron is used as 7 eV [20] and assumed  $I = A$  for iron, global hardness of  $\text{Fe} = 0$  [21]. The  $\Delta N$  can be calculated based on equation 4.

$$\Delta N = \frac{\chi_{\text{Fe}} - \chi_{\text{inb}}}{2(\eta_{\text{Fe}} + \eta_{\text{inb}})} \quad 4$$

Analysis of information on the active side of molecular inhibitors was carried out by calculating the value of Fukui indices. Fukui function is defined as [22]:

$$f = \left( \frac{\partial p(\vec{r})}{\partial N} \right)_{v(\vec{r})} \quad 5$$

Where  $p(\vec{r})$ ,  $N$ ,  $v(\vec{r})$  are first derivatives of electron density, the number of electrons, constant external potential, respectively. Using another approach, Fukui function can be measured for nucleophilic attacks as follows [23]:

$$f^+ = q(N+1) - qN \quad 6$$

and for electrophilic attack:

$$f^- = qN - q(N-1) \quad 7$$

where,  $q$  represents the total charge of the atomic inhibitor,  $q(N+1)$  the cation charge,  $qN$  the charge of neutral molecules and  $q(N-1)$  is the charge of the anionic form. Mulliken population analysis underlies the Fukui indices calculation in this study.

The electron donation intensity from the active side of the atom inhibitor was studied further using Natural Population Analysis (NBO) in terms of the second order interaction energy ( $E_2$ ).  $E_2$  describes the intensity of each electron donor between the Lewis Donor (i) and non-Lewis Acceptor NBO (j).  $E_2$  associated with  $i \rightarrow j$  delocalization can be estimated as follows [24]:

$$E2 = qi \frac{F(i,j)}{\epsilon_i - \epsilon_j}$$

8t

Here,  $qi$  is the donor orbital occupancy,  $\epsilon_i$ ,  $\epsilon_j$  are diagonal elements (orbital energies), and  $F(i,j)$  are off-diagonal elements, respectively, associated with the NBO Fock matrix.

## RESULTS AND DISCUSSION

Two different groups are selected as substituents of benzyl nicotine (BN) inhibitors to provide a stronger electronic effect. Electron donating ( $\text{CH}_3$ ,  $\text{NH}_2$ ,  $\text{OH}$ , and  $\text{CH}_2\text{OH}$ ) and withdrawing groups ( $\text{Cl}$ ,  $\text{COOH}$ , and  $\text{NO}_2$ ) are added to the carbon position in the benzyl nicotine section. The structure of benzylnicotine with its derivatives is depicted in Figure 1.

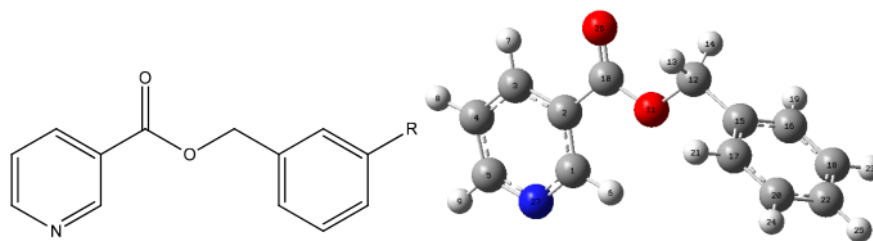


**FIGURE 1.** a. Benzylnicotine structure  $R = \text{CH}_3$ ,  $\text{NH}_2$ ,  $\text{OH}$ ,  $\text{CH}_2\text{OH}$ ,  $\text{Cl}$ ,  $\text{COOH}$ , and  $\text{NO}_2$ ; b. Optimized structure of benzylnicotine by DFT B3LYP/6-311++G(d,p)

As a consequence of the selection of the DFT and MP2 methods, it is necessary to do a basis set selection to measure the accuracy of molecular modeling calculations. The validation stage of this method is done by measuring the suitability of the experimental benzylnicotine crystal structure [25] with theoretical studies. Table 1 shows the geometric parameters of optimized structure benzylnicotine. The compatibility of bond distance and the bond angle between experimental and theoretical studies can be seen in Table 1. Linear correlation between experimental and theoretical results is fulfilled, the bond length is only different from 0.01 Å as well as the bond angle between experiment and theoretical, so the chosen basis set of 6-311++G (d,p) can be used for the studied system.

Quantum parameters can be used to predict more efficient compounds as corrosion inhibitors. Substituent effects on the inhibitory efficiency of benzyl nicotine and its derivatives can be seen in Tables 2 and 3. Experimental studies on corrosion inhibition efficiency of iron benzyl nicotine in iron showed an efficiency value of 90.8% measured using the method of weight loss. Table 2 and 3 showed that the addition of the  $\text{NH}_2$  electron donor group increases efficiency by 18%. In contrast, the addition of the  $\text{NO}_2$  an electron withdrawing group reduces inhibition efficiency by 6%. This trend is related to the energy values of HOMO and LUMO on inhibitor molecules.

The greater the energy of HOMO or the smaller the energy of LUMO, the stronger the organic molecule is attached to the metal surface. These organic molecules will have high inhibitory efficiency. The HOMO energy shows the nature of molecules to donate electrons, while LUMO energy shows the nature of molecules to accept electrons [19,26-28]. The HOMO energy values of BN- $\text{NH}_2$  and BN- $\text{NO}_2$  calculated by B3LYP/6-311++G(d,p) method are -5.9734 eV and -7,643 eV, respectively. The presence of  $\text{NO}_2$  substituents slows down the reactivity of the benzene ring and causes the benzene ring bond with the metal to be broken. The addition of  $\text{NO}_2$  substituents is predicted to have a less effect on the efficiency of corrosion inhibition. The same trend is also found in the results of MP2/6-311G(d, p) where the HOMO energy values of BN- $\text{NH}_2$  is -8.16062 eV greater than the BN-  $\text{NO}_2$  energy of -9.856 eV.

Inhibition efficiency is also influenced by other quantum parameters such as electronegativity, ionization potential, electron affinity, and electron transfer. The small value of electronegativity causes the molecules to easily reach electron equilibrium so that it becomes more unreactive while the high electronegativity value indicates the opposite [29-31]. Table 2 and 3 showed that the BN- $\text{NH}_2$  electronegativity value is 3.908 eV whereas BN- $\text{NO}_2$  is 5.3606 eV with the DFT method. The MP2 method obtained the electronegativity values of BN- $\text{NH}_2$  and BN- $\text{NO}_2$  of 3.0722 eV and 4.4737 eV, respectively. Therefore, it can be predicted that the addition of BN- $\text{NH}_2$  has higher inhibition efficiency than the addition of BN- $\text{NO}_2$  because BN- $\text{NH}_2$  is easier to achieve electron equilibrium.

2

The ionization potential (I) can also be used to measure the reactivity of atoms or molecules. High ionization potential values indicate that molecules have low reactivity or chemical inertness; whereas low ionization potential values indicate molecules have high reactivity [29-31]. Tables 1 and 2 also show patterns of increase in ionization potential that follow the pattern of increasing HOMO energy. The ionization potential value of addition of NH<sub>2</sub> with the DFT method is 5.9734 eV lower than the ionization potential value for NO<sub>2</sub> increase which is 7.6423 eV, whereas with the MP2 method the added value of ionization potential is addition of NH<sub>2</sub> and NO<sub>2</sub> of 8.1606 eV and 9.8560 eV, respectively. Based on this data, it can be predicted that the addition of NH<sub>2</sub> has higher inhibition efficiency than the addition of NO<sub>2</sub>.

The electron transfer value is the quantity of electrons transferred by organic compounds to the metal surface. Judging from the data in Table 1 and 2, the addition of NO<sub>2</sub> has a lower electron transfer than NH<sub>2</sub> so that the inhibitory efficiency is also lower. The transfer electron value of adding NH<sub>2</sub> with the DFT method is 0.7485 while the addition of NO<sub>2</sub> is 0.3592. The MP2 method shows electron transfer values for addition of NH<sub>2</sub> and NO<sub>2</sub> of 0.3860 and 0.2347, respectively. The corrosion efficiency inhibition increases with increasing electron transfer value, because the more electrons are transferred to the surface, the more electrons coat the metal surface, so that the corrosion process can be inhibited. The value of  $\Delta N$  is directly proportional to the energy value of HOMO and LUMO, ionization potential, electron affinity and electronegativity.

**TABLE 1.** Geometric parameters of benzylnicotine based on experimental and theoretical calculations B3LYP/6-311++G(d,p)

Bond distance	Exp* (Å)	Theory (Å)	Bond Angle	Exp* (Å)	Theory (Å)
C1-C2	1.394	1.4010	N27-C1-H6	116.40	116.4776
C1-N27	1.331	1.3372	C1-C2-C3	117.80	118.3073
C1-H6	1.089	1.0864	C1-C2-C10	122.70	123.0509
C2-C3	1.387	1.3991	C2-C3-H7	118.60	119.1619
C2-C10	1.502	1.4907	C4-C3-H7	121.20	122.1683
C3-C4	1.383	1.3902	C3-C4-H8	120.90	121.2411
C3-H7	1.081	1.0854	C5-C4-H8	119.70	120.3981
C4-C5	1.358	1.3972	C4-C5-H9	119.50	120.2591
C4-H8	1.079	1.0850	N27-C5-H9	114.70	115.8617
C5-N27	1.314	1.3395	C5-N27-C1	117.10	117.2617
C5-H9	1.086	1.0889	C2-C10-O25	122.80	123.0153
C10-O25	1.209	1.2160	C2-C10-O11	112.10	112.2943
C10-O11	1.339	1.3493	C10-O11-C12	114.90	115.5285
C12-O11	1.452	1.4545	O11-C12-H13	107.50	108.2535
C12-H13	1.089	1.0939	O11-C12-H14	107.90	108.3835
C12-H14	1.088	1.0938	C15-C12-H13	112.10	112.1611
C12-C15	1.501	1.5036	C15-C12-H14	111.90	112.0533
C15-C16	1.387	1.3996	C15-C16-H19	118.80	119.4821
C15-C17	1.401	1.4005	C15-C16-C18	119.90	120.5975
C16-H19	1.085	1.0875	C15-C17-H21	118.50	119.4840
C16-C18	1.389	1.3952	C15-C17-C20	120.30	120.5783
C17-H21	1.085	1.0875	C16-C18-H23	119.60	119.8821
C17-C20	1.378	1.3944	C18-C16-H19	119.70	119.9212
C18-C22	1.386	1.3959	C18-C22-H25	120.10	120.0853
C18-H23	1.082	1.0863	C18-C22-C20	118.90	119.8521
C20-C22	1.384	1.3966	C17-C20-H24	118.80	119.8864
C20-H24	1.083	1.0866	C20-C22-H25	119.70	120.0640
C22-H25	1.085	1.0867	C22-C20-H24	119.90	120.1137

**TABLE 2.** Quantum parameters and the inhibition efficiency of corrosion of benzyl nicotine and its derivatives are calculated using DFT B3LYP/6-311++G(d,p).

Inhibitors	Parameters							
	$E_{\text{HOMO}}$ (eV)	$E_{\text{LUMO}}$ (eV)	$E_{\text{gap}}$ (eV)	$I$ (eV)	$A$ (eV)	$\chi$ (eV)	$\Delta N$	%IEtheory
BN	-7.2254	-1.9535	-5.2719	7.2254	1.9535	4.5895	0.4572	90.8000
BN-CH <sub>2</sub> OH	-6.8741	-1.9274	-4.9468	6.8741	1.9274	4.4008	0.5254	95.2147
BN-CH <sub>3</sub>	-6.8752	-1.9255	-4.9498	6.8752	1.9255	4.4004	0.5252	95.2010
BN-COOH	-7.4845	-2.1198	-5.3647	7.4845	2.1198	4.8021	0.4097	87.5446
BN-Cl	-7.0894	-2.0645	-5.0249	7.0894	2.0645	4.5770	0.4822	92.6839
BN-NH <sub>2</sub>	-5.9734	-1.8425	-4.1310	5.9734	1.8425	3.9080	0.7485	107.524
BN-NO <sub>2</sub>	-7.6423	-3.079	-4.5634	7.6423	3.0790	5.3606	0.3592	84.7436
BN-OH	-6.5337	-1.9415	-4.5922	6.5337	1.9415	4.2376	0.6015	98.3954

**TABLE 3.** Quantum parameters and benzylnicotine corrosion inhibition efficiency and derivatives are calculated using MP2/6-311++G(d,p)

Inhibitors	Parameters							
	$E_{\text{HOMO}}$ (eV)	$E_{\text{LUMO}}$ (eV)	$E_{\text{gap}}$	$I$ (eV)	$A$ (eV)	$\chi$ (eV)	$\Delta N$	%IEtheory
BN	-9.3362	1.9946	-11.3308	9.3362	-1.9946	3.6708	0.2938	90.8000
BN-CH <sub>2</sub> OH	-7.9386	3.8966	-10.8352	6.9386	-3.8966	1.5210	0.5057	96.2089
BN-CH <sub>3</sub>	-8.8737	2.128	-11.0017	8.8737	-2.1280	3.3729	0.3297	84.8844
BN-COOH	-7.7961	5.3715	-13.1676	7.7961	-5.3715	1.2123	0.4395	96.1886
BN-Cl	-9.603	1.8476	-11.4506	9.6030	-1.8476	3.8777	0.2727	93.5938
BN-NH <sub>2</sub>	-8.1606	2.0163	-10.1769	8.1606	-2.0163	3.0722	0.3860	75.2019
BN-NO <sub>2</sub>	-9.856	0.9087	-10.7647	9.8560	-0.9087	4.4737	0.2347	64.8974
BN-OH	-8.7457	2.000	-10.7457	8.7457	-2.0000	3.3729	0.3375	53.9336

Linear correlation between quantum parameters and corrosion inhibition efficiency of nicotine benzyl compounds and their derivatives can be seen in Figure 2. Linear correlation between HOMO energy, ionization potential, electronegativity, and electron transfer with corrosion inhibition efficiency seen from the regression value  $r^2$  of 0.99264, 0.99264, 0.8639 and 0.9951, respectively. Figure 2 shows that if the HOMO value is higher, the corrosion inhibition efficiency increases. The lower the ionization potential, the inhibition efficiency also increases. Furthermore, if electronegativity gets lower and the electron electron transfer increases, the efficiency of corrosion inhibition increases. Visualization of structural optimization, HOMO and LUMO energy, electromagnetic potential of benzylnicotine compounds can be seen in Figure 3. Electrostatic potential surface (ESP) is an opportunity to find the distribution of electron charge in the cartesian coordinates (x, y, and z) in a molecule. ESP is related to electron density, an area where electrons can be found to explain molecular properties, predict molecular structure, bond strength, reactivity and molecular stability. The EPS value shows the active side of benzylnicotine in aromatic regions that have heteroatoms

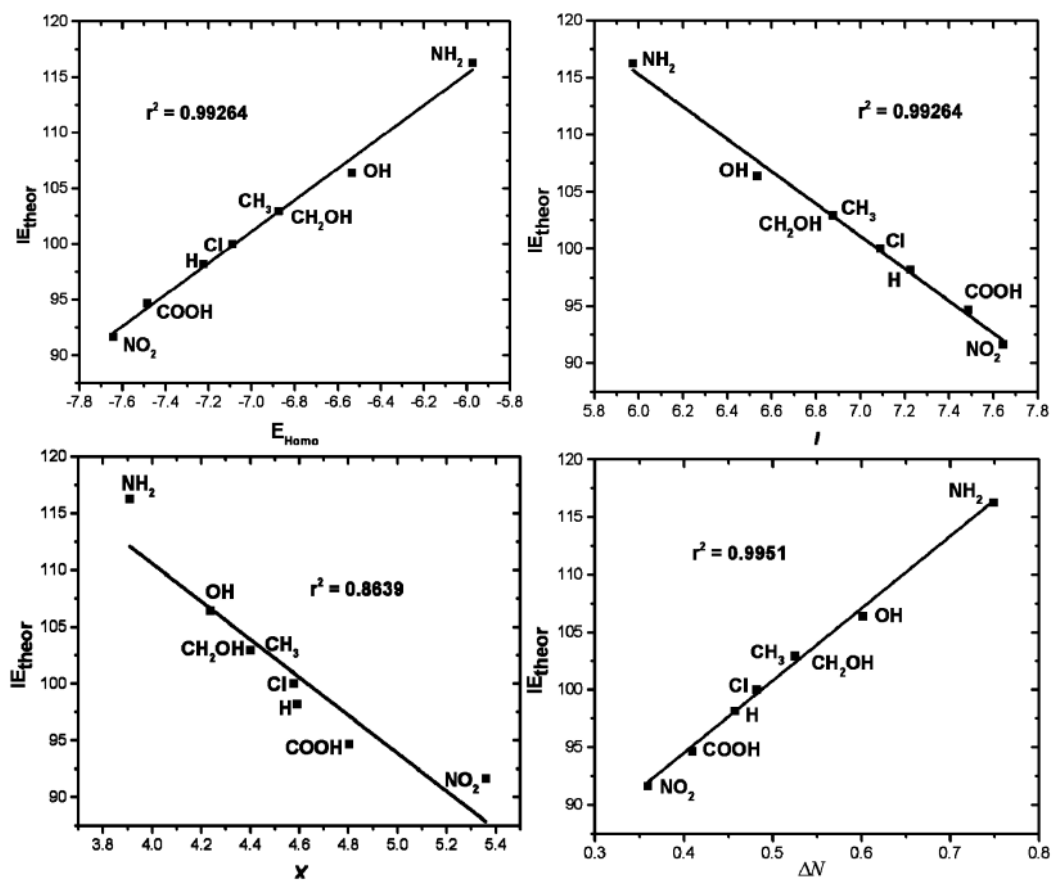
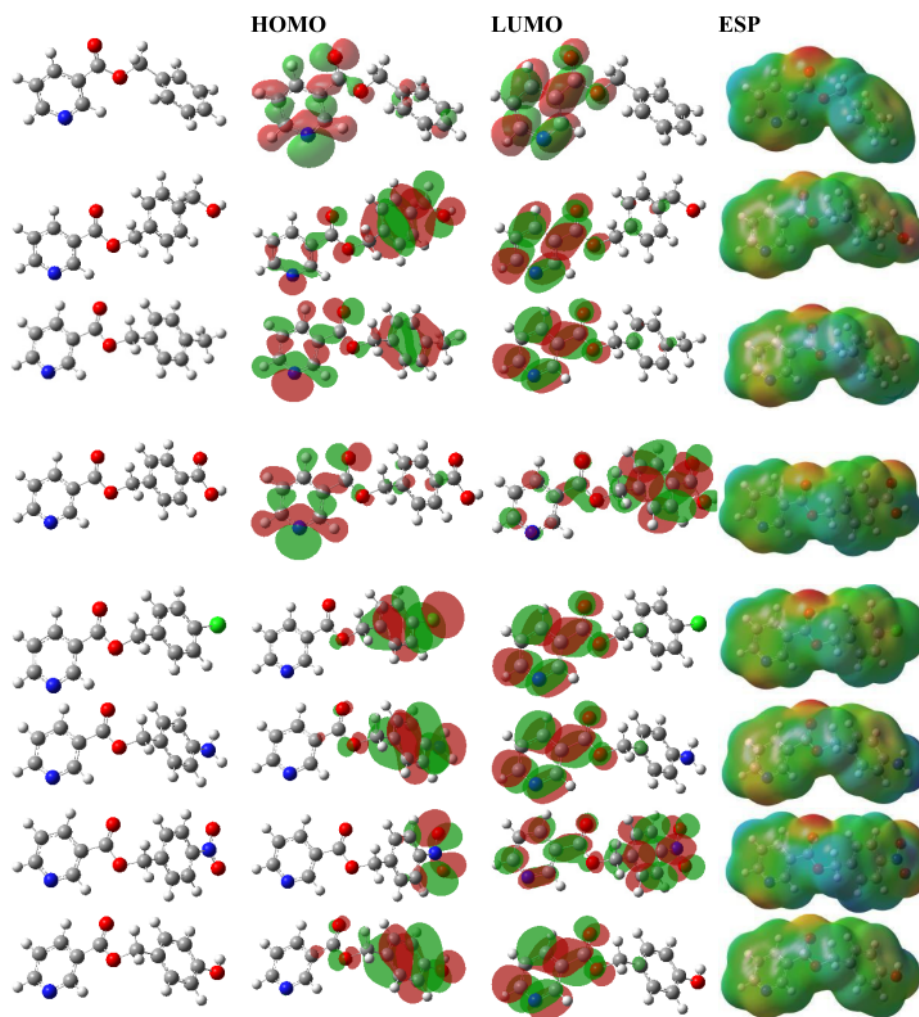


FIGURE 2. Correlation between the efficiency of corrosion inhibition (%IE) and quantum parameters such as HOMO energy, ionization potential, electronegativity and electron transfer.





**FIGURE 3.** Visualization of HOMO-LUMO energies and electrostatic potential of benzylnicotine and its derivatives

Each molecule has an active side that is used in interacting. To find out the point where a molecule donates an electron or receives an electron can be predicted using the analysis of the Fukui function. Changes in electron density are explained in nucleophilic form  $f^+$  and electrophilic  $f^-$ . The value of  $f^+$  is an electron deficit area, indicating the ability of atoms to accept electrons which are back donations from metal. Whereas  $f^-$  is an electron-rich region, indicating the ability of atoms to donate electrons to empty d orbitals in metal [31]. Tables 4 show Fukui values of nicotine benzyls and their derivatives, where it can be seen that C3 and C5 carbon atoms act as nucleophilic because they have a high  $f^+$  value so they are susceptible to receiving electrons from metals. Atoms that act electrophilic attacks are C2 and N6 which can donate electrons to the metal surface, this is indicated by a high value of  $f^-$ -atom.

**TABLE 4.** Fukui values for nucleophilic and electrophilic attack of benzyl nicotine and its derivatives using the DFT B3LYP/6-311++ G(d,p) method

Compounds	Atom	N (-1)	N (0)	N(+1)	f(-)	f(+)
BN-NH <sub>2</sub>	C1	-0.2117	-0.1801	-0.2166	0.0316	-0.0365
	C2	1.0640	1.0953	1.0655	0.0314	-0.0298
	C3	0.1707	0.3315	0.3844	0.1608	0.0529
	C4	-0.0382	0.0077	0.0472	0.0460	0.0395
	C5	-0.2714	-0.1261	-0.0860	0.1452	0.0401
	N6	-0.0731	-0.0243	0.0302	0.0488	0.0545
BN-NO <sub>2</sub>	C1	-0.2494	-0.2643	-0.2575	-0.0149	0.0068
	C2	0.8342	0.8265	0.8465	-0.0078	0.0200
	C3	0.3629	0.4481	0.5599	0.0851	0.1118
	C4	-0.0733	-0.0370	0.0408	0.0363	0.0778
	C5	-0.1860	-0.1016	-0.0415	0.0845	0.0601
	N6	-0.0520	-0.0196	0.1450	0.0323	0.1646

**TABLE 5.** Second-order interaction energy (E2) kcal.mol<sup>-1</sup> from benzyl nicotine and its derivatives by MP2/6-311++G(d,p) method

Compounds	Donor	Acceptor	E2
BN	LP(1) N27	LP*(7) Fe28	5.67
	LP(1) Fe28	RY*(1)N27	0.28
	LP(2) Fe28	RY*(3)C2	1.06
BN-CH <sub>2</sub> OH	LP(1) N6	LP*(7)Fe 32	5.66
	LP*(4)Fe 32	RY* (1) N6	0.58
	LP(2) Fe32	RY* (3) C2	1.09
BN-CH <sub>3</sub>	LP(1) N6	LP* (7) Fe31	5.64
	LP(1) Fe31	RY* (1) N6	0.58
	LP(2) Fe31	RY* (3) C2	1.09
BN-COOH	LP(1) N6	LP*(7) Fe31	5.63
	LP(4) Fe31	RY* (1) N6	0.57
	LP(3) Fe31	RY* (1) C5	1.05
BN-NH <sub>2</sub>	LP(1) N6	LP*(7) Fe 30	6.03
	LP(1) Fe30	RY* (1) N6	0.59
	LP(2) Fe30	RY* (3) C2	1.09
BN-NO <sub>2</sub>	LP(1) N6	LP*(8) Fe30	5.61
	LP(1) C5	LP*(5) Fe30	25.83
	LP(3) Fe 30	RY* (1) N6	0.55
	LP(3) Fe30	LP(1) C5	5.83
BN-OH	LP(1) N6	LP*(7) Fe 30	5.67
	LP(1) Fe30	RY* (1) N6	0.59
	LP(2) Fe30	RY* (3) C2	1.08
BN-Cl	LP(1) N6	LP* (7) Fe 28	5.63
	LP*(4) Fe28	RY* (1) N6	0.57
	LP(3) Fe28	RY* (1) C5	1.05

The effect of electron donor-acceptor substituents was further studied using second-order energy interaction (E2) based on analysis of Natural Bonding Orbital (NBO) [24]. The E2 value obtained from the NBO analysis uses the DFT method shown in Table 5. The values selected for second-order interactions show the interaction between a single electron pair (LP) of nitrogen and carbon with a single electron antibonding (LP\*) pair of Fe indicating the presence of second-order interaction energy (E2). The second-order interaction energy (E2) for the maximum donor between Fe and benzyl nicotine with the addition of NH<sub>2</sub>, OH, CH<sub>2</sub>OH, CH<sub>3</sub>, BN, Cl, COOH and NO<sub>2</sub> substituents

respectively is 5.23, 5.21, 5.21, 5.19, 5.17, 5.17, 5.16 and 4.47 kcal.mol<sup>-1</sup>. The E2 value can also be used to explain why NH<sub>2</sub> has the highest inhibition efficiency. Addition of NH<sub>2</sub> substituents has the highest E2 value and increases corrosion inhibition efficiency. In addition to donating electrons, nitrogen atoms also receive electrons back from iron, even though the E2 value is small. Thus, it can be concluded that the result of the second order interaction energy value (E2) corresponds to the quantum parameter descriptor and function analysis of Fukui. The NBO analysis uses DFT and the MP2 method shows results that are not much different, MP2 gives a slightly higher value than the DFT. The values chosen for second-order interactions show the interaction between a single electron pair (LP) of nitrogen and carbon with a single electron antibonding (LP) pair of Fe which indicates the presence of second-order interaction energy (E2).

## CONCLUSION

Density functional theory and MP2 has been used to examine the effect of substituents on the inhibition efficiency of benzyl nicotine and its derivatives. The driving group of electrons increases the efficiency of inhibition of benzyl nicotine and the electron pulling group has the opposite effect. Analysis of the Fukui indices and second order energy interaction (E2) also succeeded in predicting the active side of the benzyl nicotine compound and its derivatives. Nitrogen and the aromatic benzene group are the most active side of the benzyl nicotine compound which can play a role in donating electrons to the metal and simultaneously contributing to receiving electron back contributions from metals. Linear correlation is shown between inhibition efficiency and quantum parameters. This theoretical study shows that substituents influence the efficiency of corrosion inhibition.

## ACKNOWLEDGMENT

Financially supported by Kemenristekdikti Indonesia melalui Penelitian Dasar tahun 2019, Grant Number: 1826/UN18.L1/PP/2019, is gratefully acknowledged.

## REFERENCES

1. M. E. Belghiti, S. Echih, A. Dafali, Y. Karzazi, M. Bakasse, H. Elalaoui-Elabdallaoui, M. Tabyaoui, *Applied Surface Science*, **491**, 707-722 (2019).
2. J. Mao, X. He, Y. Tang, *Corrosion Science*, **148**, 171-177 (2019).
3. H. Ju, & Y. Li. *Corrosion Science*, **49**(11), 4185-4201 (2007).
4. Vinutha, M. R, T. V. Veenkatesha, and B. Vinayak. *Portugalia ElectrochimicaActa*. **35**(5), 253-268 (2017).
5. D. K. Singh, S. Kumar, G. Udayabhanu, & R. P. John. *Journal of Molecular Liquids*, **216**, 738-746 (2016).
6. S. Hadisaputra, A. A. Purwoko, S. Hamdiani, & N. Nuryono. In *IOP Conference Series: Materials Science and Engineering* 509(1), p. 012129 IOP Publishing. (2019).
7. C. Verma, M. A. Quraishi, I. B. Obot, & E. E. Ebenso. *Journal of Molecular Liquids*, **287**, 110972 (2019).
8. S. Hamdiani, I. H., Rohimah, Nuryono, A. A., Purwoko, L. R. T. Savalas, S. Hadisaputra, *Asian Journal of Chemistry* **31** (3), 555-558. (2019).
9. I. Abdulazeez, A. Zeino, C. W. Kee, A. A. Al-Saadi, M. Khaled, M. W. Wong, & A. A. Al-Sunaidi. *Applied Surface Science* **471** 494-505. (2019).
10. S. Hadisaputra, A. A. Purwoko, S. Hamdiani, and Y. P. Prananto, *IOP Conference Series: Materials Science and Engineering* **546** 3, p. 032011. IOP Publishing. (2019).
11. B. S. Hou, N. Xu, Q. H. Zhang, C. J. Xuan, H. F. Liu, & G. A. Zhang. *Journal of the Taiwan Institute of Chemical Engineers*, **95**, 541-554 (2019).
12. S. Hadisaputra, S. Hamdiani, M. A. Kurniawan, and N. Nuryono. *Indonesian Journal of Chemistry*, **17**(3), 431-438 (2017).
13. S. Hadisaputra, A. A. Purwoko, I. Ilhamsyah, S. Hamdiani, D. Suhendra, N. Nuryono, B. Bundjali, *International Journal Of Corrosion And Scale Inhibition* **7** (4), 633-647 (2018).
14. M. J. Frisch,; G. W. Trucks, H. B. Schlegel, G. E. Scuseria, M. A. Robb, K. N. Kudin, M. C. Strain, O. Farkas, J. Tomasi, V. Barone, M. Cossi, R. Cammi, B. Mennucci, C. Pomelli, C. Adamo, S. Clifford, J. Ochterski, G.A. Petersson, P. Y. Ayala, Q. Cui, K. Morokuma, D.K. Malick, A. D. Rabuck, K. Raghavachari, J. B. Foresman, J. Cioslowski, J. V. Ortiz, B. B. Stefanov, G. Liu, A. Liashenko, P. Piskorz, I. R. Komaromi, R. Gomperts, L. Martin, D. J. Fox, T. Keith, M. A. Al-Laham, C.Y. Peng, A. Nanayakkara, C. Gonzalez, M. P.

- Challacombe, M. W. Gill, B. Johnson, W. Chen, M. W. Wong, J. L. Andres, C. Gonzalez, M. Head-Gordon, E.S. Replogle, Pople. J.A. Gaussian 09; Gaussian, Inc. Wallingford, CT, **2009**
15. S. Hadisaputra, H. D. Pranowo, & R. Armunanto. *Indonesian Journal of Chemistry*, **12**(3), 207-216 (2012).
  16. S. Hadisaputra, L. R. Canaval, H. D. Pranowo, & R. Armunanto. *Monatshefte für Chemie-Chemical Monthly*, **145**(5), 737-745 (2014).
  17. S. Hadisaputra, L. R. Canaval, H. D. Pranowo, & R. Armunanto. *Indonesian Journal of Chemistry*, **14**(2), 199-208 (2014).
  18. Luo, X., Ci, C., Li, J., Lin, K., Du, S., Zhang, H., & Liu, Y. *Corrosion Science*, **151**, 132-142 (2019).
  19. Lukovits, E. Kalman, F. Zucchi,. *Corrosion*, **57**(1), 3-8. (2001)
  20. S. Martinez. *Materials Chemistry and Physics*, **77**(1), 97-102. (2002).
  21. M. J. S. Dewar, W. Thiel. *Journal of American Chemical Society*. **85**, 3533 (1963)
  22. F. De Proft, J.M.L. Martin, P. Geerlings Calculation of molecular electrostatic potentials and Fukui functions using density functional methods *ChemPhysLett*, **256** pp. 400-408 (1996).
  23. R. R. Contreras, P. Fuentealba, M. Galván, P. Pérez. *ChemPhysLett*, **304** (1999), pp. 405-413
  24. Weinhold. *Journal of computational chemistry*, **33**(30), 2363-2379 (2012)
  25. R. K. McMullan, J. Epstein, J. R. Ruble, & B. M. Craven. (1979). *Acta Crystallographica Section B: Structural Crystallography and Crystal Chemistry*. **35**(3), 688-691 (1979).
  26. S. Hadisaputra, S. Hamdiani, M. A. Kumiawan, and N. Nuryono. *Indonesian Journal of Chemistry*, **17** 3 431-438 (2017) .
  27. S. Hadisaputra, A. Purwoko, F. Wajdi, I. Sumarlan, S. Hamdiani. *International Journal of Corrosion and Scale Inhibition*, **8**(3) 673-688 (2019).
  28. A. Popova, M. Christov, T. Deligeorgiev, Influence of the molecular structure on the inhibitor properties of benzimidazole derivatives on mild steel corrosion in 1 M hydrochloric acid. *Corrosion*. **59**(9), 756-764. (2003).
  29. P. Politzer, L. Abrahmsen, & P. Sjöberg, P. *Journal of the American Chemical Society*, **106**(4), 855-860 (1984).
  30. V. K. Turchaninov, E. A. Motvienko, L. I. Larina, A. M. Shulunova, L. V. Baikalova, & V. A. Lopyrev, The study of benzimidazoles. *Russian Chemical Bulletin*, **42**(10), 1683-1689 (1993).
  31. L. Pauling. *The Nature of the Chemical Bond*, Cornell University Press, Ithaca, New York. (1960).

ORIGINALITY REPORT

**20%**  
SIMILARITY INDEX

**21%**  
INTERNET SOURCES

**14%**  
PUBLICATIONS

**3%**  
STUDENT PAPERS

PRIMARY SOURCES

**1** [ijcsi.pro](http://ijcsi.pro) Internet Source **7%**

**2** [www.researchgate.net](http://www.researchgate.net) Internet Source **6%**

**3** [eprints.unram.ac.id](http://eprints.unram.ac.id) Internet Source **3%**

**4** Submitted to Universitas Diponegoro Student Paper **3%**

Exclude quotes Off

Exclude matches < 3%

Exclude bibliography Off

# B22

---

## GRADEMARK REPORT

---

FINAL GRADE

GENERAL COMMENTS

**/0**

**Instructor**

---

PAGE 1

---

PAGE 2

---

PAGE 3

---

PAGE 4

---

PAGE 5

---

PAGE 6

---

PAGE 7

---

PAGE 8

---

PAGE 9

---

PAGE 10

---

PAGE 11

---